DOI 10.31489/2022Ph1/58-67

UDC 620.192:534 – 16:53.887.45

A.A. Bespal'ko[1*], G.E. Utsyn[2], P.I. Fedotov[1]

[1]*National Research Tomsk Polytechnic University, Tomsk, Russia*
[2]*Tomsk State University of Control Systems and Radioelectronics, Tomsk, Russia*
(E-Mail: besko48@tpu.ru)

Experimental Studies of Mechanical-Electrical Transformations during the Destructive Processes Developing in Dielectric Materials

A mechanical-electrical method for testing fractures developing within the stress-strain state changes of dielectric rock samples, as an example, is discussed here. The paper discusses the results of numerical and experimental studies of changes in the electromagnetic responses parameters under the pulse deterministic acoustic excitation of rock samples with different composition and texture. The paper presents the results of mathematical calculations of the stress concentration on cracks located along and across the sample axis, perpendicular to which deterministic acoustic pulses were introduced. The cracks presented in the sample volume are stress concentrators. With a different number and sizes of cracks perpendicular to the propagation of an acoustic pulse, the intensity of stresses and their type differ significantly. This circumstance indicates the influence of the structure of the samples and their dielectric properties on the parameters of electromagnetic signals when recording the results of mechanical and electrical transformations. Thus, the use of the method of mechanical-electrical transformations under compression can be used in testing the processes of the onset of crack formation and the development of fracture in solid-state dielectric materials and products.

Keywords: dielectrics, rocks, numerical modeling, acoustic impact, uniaxial compression, electromagnetic emission, mechanoelectric transformations, electromagnetic signal.

Introduction

The development of destruction of solid dielectric structures is accompanied by occurrence of alternating electromagnetic fields. This phenomenon is being addressed to employ the parameters and characteristics of electromagnetic emission for testing imperfection and to study development of destruction of solid dielectric materials. Alternating electromagnetic fields arise from mechanical-electrical transformations (MET) in solid-state structures when their stress-strain state changes under mechanical load with subsequent acoustic emission inside the test material. Electromagnetic radiation due to various types of destruction mechanisms has been proven to emerge in all-dielectric materials [1–12]. During MET processes, electromagnetic signals (EMS) are generated due to the changed charge state of materials or their interfaces. The presence, occurrence, and quantitative or qualitative change of electric charges and their vibrations under acoustic excitation are a prerequisite for EMS generation.

In [13], the issues of charging layers of rocks of different textures and compositions are considered in detail. In [3], Khatiashvili and Perelman experimentally and theoretically proved that acoustic wave-induced generation of EMS, which is a consequence of the oscillatory movements of double electric layers and fluctuation-charged edges of microcracks, and release and vibration of charged dislocations. EMS parameters depend on the amplitude-frequency spectrum of the acoustic field excited by linear deformations of the sources.

Mechanisms of EMS generation and source types were summarized to distinguish processes that induce separation of electric charges and form electric dipoles. These processes include: uneven distribution of electric charges on crack edges when ionic or other types of bonds are broken; in inhomogeneous field of mechanical stresses, charged defects start to migrate in the area of crack formation; at the interface of mineralized water released during heating with the rock; friction-induced electrification during movement of structural elements. On the other hand, the change in the dipole moment is determined by the breakdown between the charged sides of the crack, charge relaxation if the current flows through the dielectric body outside the crack; electron emission; vibrations of charged surfaces.

Thus, EMS generation is due to the change in the charge state of the test material during development of cracks of various scales or double electric layers at the interface of media, minerals, and aqueous solutions. During crack development, acoustic emission methods can be employed, which use acoustic pulses emitted by growing cracks of different lengths and record electromagnetic signals when the charged edges of these cracks vibrate. These are mechanical-electrical methods.

Experimental

Experimental studies of mechanical and electrical transformations were carried out on samples of rocks from the Tashtagol iron ore deposit, which have different ratios of magnetite and calcite. These minerals are distinguished by their ultimate strength: $(12–50)\times10^6$ Pa - for calcite [14]; $(14\text{-}21.5)\times10^7$ Pa - for magnetite ore and skarns of the Tashtagol deposit, calculated from the date of destruction of samples in experiments. In addition, calcite and magnetite differ significantly in their electrical characteristics. So the specific electrical resistance(ρ) of calcite is (10^7 - 10^{12}) Ohm · m, and magnetite is (10^{-5} - 10^4) Ohm·m [14, 15]. The magnetite content in the ore samples used ranged from 60 to 77 percent. In addition, skarn samples containing magnetite were used. Samples for experiments were made from cores with a diameter of $(42 \pm 1)\times10^{-3}$ m and a length of $(80 \pm 5)\times10^{-3}$ m.

Investigations of the electromagnetic emission (EME) characteristics under uniaxial compression loads were carried out on the stand, the block diagram of which is shown in Figure 1. In the course of the experiment, the sample was placed between the support (1) and the movable plate (2) of the IP500.1 automated press, which developed the force P on the sample up to 500 kN.

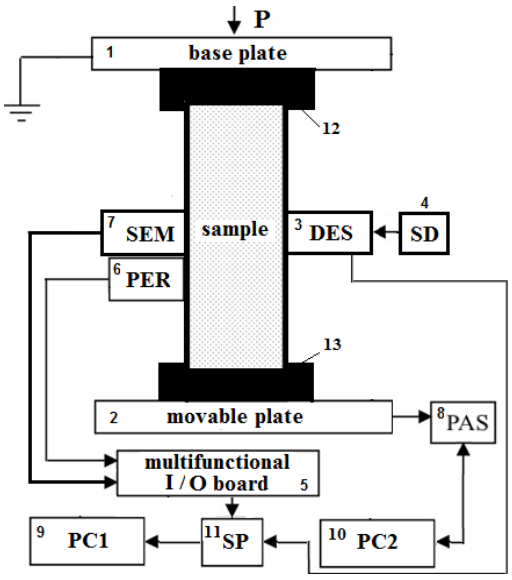

1 — base plate of the IP500.1 press; 2 — movable press plate IP500.1; 3 — dynamic excitation system to control the energy of the impact of the ball; 4 — spring device PU for accelerating the ball for introducing a deterministic acoustic pulse into the sample; 5 — multifunctional input-output board NI BNC 2120; 6 — PER piezoelectric receiver; 7 — electromagnetic differential capacitive sensor; 8 — press automatic system; 9 — personal computer PC1 for visualization and amplitude-frequency analysis of acoustic and electromagnetic signals; 10 — personal computer PC2 for operating with the press; 11 — software block; 12, 13 — holders for centering the sample.

Figure 1. Block diagram of the stand for uniaxial compression of the test samples.

The load and loading rate of the sample was set using a specialized program from a PC2 computer (10) through the press automatic system (8) to the actuator of the servo valve. Moreover, changes in the load could be set linear, stepwise, or cyclical. For centering the samples, special holders 12 and 13 were used. Recording of information on changes in the sample deformation due to applied forces and their type was recorded and displayed on the PC2 computer monitor. Uniaxial compression was carried out at a constant rate of 0.3 Pa/s. Acoustic impulse excitation of the samples by the impact of the ball was carried out using a spring device for accelerating the impacting ball SD (4) through the impact energy control system DES (3) [12, 23]. The shape of the acoustic pulse was close to the bell-shaped Gaussian distribution, and its duration at the 0.1 of maximum amplitude was 50×10^{-6} seconds. A point impact with a ball weighing 8.6×10^{-4} kg was applied in the middle of the free cylindrical part of the sample. After flying through 3, the ball hit a hardened steel plate 2×10^{-3} meters thick, excited a deterministic acoustic pulse, which passed through a layer of mineral oil between the plate and the sample into the sample. The hardness of the steel of the plate and the ball were of equal values. The residual impact energy introduced into the sample after the ball bounced was $(5 ... 30)\times10^{-3}$ J. The acoustic signal, passing through the sample, was recorded by the PER piezoelectric acoustic pulse receiver (6).

The DES system comprised a metal tube with two optical pairs built into it at a distance of 5×10^{-2} meters, each of which included a light-emitting diode (LED) and a photodiode. The ball, flying through the optical pairs, gave two marks on the PC1 computer monitor (9). These marks were used to calculate the ball raid V_1 and V_2 rebound velocities. The calculated velocities were used to determine the kinetic energy of the acoustic impact, E_{exc}, transmitted to the sample:

$$E_{exc} = \frac{m}{2}(V_1^2 - V_2^2), \tag{1}$$

In this case, the energy losses of the acoustic pulse in the plate were not taken into account. The EMS electrical component generated by the sample during the passage of the acoustic signal was received by a differential capacitive sensor SEM (7) with a built-in power amplifier. The sensor used low and high pass filters, which ensured its operation in the range from 1 to 100 kHz. At the SEM output, the signal was amplified with a factor of 10 or 100. In the measurements, the gain was selected depending on the input EMS amplitude. The SEM input sensitivity is 5×10^{-4} V. Signals from the SEM and PER were transmitted through the NI BNC-2120 multifunctional board (5) to PC1 (9). Subsequently, using a special software program (11), the EMS amplitude was normalized to the amplitude of the acoustic pulse excited by the impact of the ball, and the EMS amplitude-frequency analysis was performed using the fast Fourier transform.

Results and Discussion

Acoustic pulses arise in the destructive zones while the material is cracking. The pulses propagation generate EMS parameters of which are depend on characteristics of the exciting acoustic pulses [2–5, 13]. Thus, the results of numerical simulation of mechanical stresses changing on cracks defects are provided here. The regularities in the EME characteristics under uniaxial compression to the destructive values of the samples were studied experimentally. These studies were carried out to determine the applicability of mechanical-electrical methods when testing the development of destructive zones and destruction in dielectric materials.

For calculations, we analyzed wave propagation in elastic inhomogeneous medium of limited dimensions with given physical and mechanical properties under pulse exposure of part of its surface. The parameters of the stress-strain state (displacement, strain, stress) were calculated. The simplest classical rigid body model was used [16–18].

The problems of wave mechanics are solved by hypotheses conventional for classical elastic medium, such as the approximation of homogeneity and continuity. Any inhomogeneity is caused by defects or inclusions that are considered explicitly, i.e., they are included in the problem statement.

For a given cylindrical magnetite ore sample, this model can be applied with some assumptions. For example, for problems related to wave propagation, it was assumed that the used samples were free of porosity, empty cavities. The study of the sample texture showed that calcite and magnetite minerals are in continuous contact and smoothly mix with each other.

The boundary conditions correspond to the laboratory experiment. Zero displacement was specified at the flat boundaries of the sample since in the laboratory experiment the sample was clamped between the punches. The side faces are free, therefore, the stresses at the boundary equal to zero. For a three-dimensional case, the free boundaries show no components of the stress vector:

$$\sigma_{\tau 1} = \sigma_{\tau 2} = \sigma_n = 0 \tag{2}$$

where σ_n is normal stresses and $\sigma_{\tau 1}, \sigma_{\tau 2}$ are tangential stresses.

In the middle of the vertical dimension of the sample $y = l$ along the normal, load is applied in the form:

$$\sigma_n = T(t) \times F(x, z),$$
$$\sigma_{\tau 1} = \sigma_{\tau 2} = 0, \tag{3}$$

where *T(t)* is a function that determines the law of load variation with time, *F(x, z)* is a function that determines the law of load variation over the surface (in a two-dimensional case along the contour line), σ_n is normal stresses and $\sigma_{\tau 1}, \sigma_{\tau 2}$ are tangential stresses, the last components of the load vector are neglected. For calculations, the dependence $T(t)$ was used in the form of a half exponentially decaying sinusoid:

$$T(t) = e^{-\beta t} \sin\left(\frac{2\pi t}{\tau}\right) \times \eta(t) \ ,$$

$$\eta(\mathrm{t}) = \begin{cases} 1.0 & \leq \ t \ \leq \ \tau \\ 0, & t \ \geq \ \tau \end{cases}, \tag{4}$$

where τ is load exposure time that depends on the duration of the deterministic acoustic pulse.

At the face end, the load was specified as a gradually increasing and then gradually decreasing function dependent on temporal and spatial coordinates. Afterpulse exposure, stresses at the upper boundary were set to zero. In calculations, the acoustic excitation pulse was close to the experimental one in shape, amplitude, and duration. In the three-dimensional case, when the load is applied to the surface, the acoustic pulse in the form of a bell-shaped function is represented as:

$$F(x,z) = A \times \exp\left(-\beta \frac{(x-x_0)^2 + (z-z_0)^2}{2d_0^2}\right), \tag{5}$$

where x_0, z_0 are the coordinates of the center of the acoustic pulse source, and d_0 is the value that determines the distance from the pulse center at which the normal stress decreases by a factor of e^{β}.

In the general case, the system of equations that describes the behavior of a deformable solid body in the spatial case includes the equations of motion

$$\rho \ddot{U}_i = \rho G_i + \sigma_{ij,j}, \tag{6}$$

where ρ is density, U_i is displacement, σ_{ij} is stresses, G_i is mass force vector components, i, j = 1, 2, 3. The dot above the symbol indicates the time derivative, and the comma after the index indicates the derivative of the corresponding coordinate. Summation is performed over the repeated indices, for example:

$$\sigma_{ij,j} = \frac{\partial \sigma_{i1}}{\partial x_1} + \frac{\partial \sigma_{i2}}{\partial x_2} + \frac{\partial \sigma_{i3}}{\partial x_3},$$

the continuity equation

$$\frac{\partial \rho}{\partial t} + \rho\left(\frac{dU_1}{dx_1} + \frac{du_2}{dx_2} + \frac{dU_3}{dx_3}\right) = 0, \tag{7}$$

where x_i is the coordinate axis.

The relation between the strain tensor components and displacements from the Cauchy relation is represented as

$$\varepsilon_{ij} = 0,5\left(U_{i,j} + U_{j,i}\right), \tag{8}$$

and the constitutive relations specify the relations between stress and strain tensor components as:

$$\sigma_{ij} = f(\varepsilon_{ij}). \tag{9}$$

In the elastic case, relations (10) are taken in the form of Hooke's law. In the applied problems of wave mechanics, the processes are described by hyperbolic equations when formulated correctly. Hyperbolic equations and systems make up a significant part of the mathematical models used to solve applied problems. A distinctive feature of hyperbolic equations and systems is that they describe wave processes with the finite rate of disturbance (wave) propagation in the considered region.

For each equation of the form

$$\frac{\partial U}{\partial t} = \frac{\partial F}{\partial x}, \tag{10}$$

the used difference scheme corresponds to the simplest version of McCormack non-central schemes [19, 20].

A volumetric design scheme was used for the equation solution. McCormack's method is a finite-difference predictor-corrector method, which refers to shock-capturing schemes. In accordance with the scheme, the position of the wavefront is not identified, and the computational domain is analyzed for each moment of time, which is needed for subsequent use of the simulation results. McCormack's scheme assumes the use of a rectangular computational grid, which has a number of advantages: simplified mathematical calculations, less computing time, simplified specification of boundary conditions, and simplified pro-

cessing of results without data loss. Results obtained by square-cell grids are best since the hourglass effect – twisting of the grid cells – is minimized. The numerical algorithm of the method is similar to the Runge–Kutta method [20] used to solve ordinary differential equations. To obtain solutions at the next time step $U(t+\Delta t)$ by the Runge-Kutta method using the known $U(t)$, one or several iterations are required.

Before using the method similar to the Runge–Kutta method of the second order of accuracy, spatial derivatives in the equations were replaced by the corresponding ratios of finite differences. Non-central difference operators were used, for example, alternately left or right differences instead of central ones. This approach forms the basis for the effective non-central second-order scheme proposed by McCormack.

Non-central schemes are superior to most conventional central schemes since the program logic is simplified, non-uniform terms are easily included, and generalization to multidimensional problems is performed directly. The advantage of non-central schemes is the absence of half-integer indices, which simplifies realization of the boundary conditions. The scheme has a second order of approximation in both spatial and temporal variables.

Thus, the boundary conditions can be specified by displacements. The size of elements in the finite element model was $(10^{-3}\times10^{-3})$ m^2. The calculation involves 237,500 points at a sampling rate of 10^{-6} s. The calculations were performed for an elastic sample of magnetite ore used in the experiments of stepwise compression and subsequent excitation at steps by deterministic acoustic pulse. Cracks specified were of different sizes with a length along the sample axis or along with the acoustic pulse propagation at the point of the ball impact. Numerical simulation was carried out using a special graphics package. The results of numerical simulation are visualized in the form of stress intensity propagation regions [21, 22]. The constructed mathematical model was used to analyze elastic wave propagation in the sample under pulsed mechanical action. This enables detailed distributions of parameters that describe the material behavior in contrast to experimental studies when the measured quantities have predominantly integral meaning. Elastic disturbances were simulated numerically in a cylindrical region, where the lateral surface was exposed to pulse excitation. It is reasonable to consider the problem in flat formulation, namely, with the axial section of the cylinder with dimensions of $(42\times80)\times10^{-6}$ m. Figure 2 shows examples of numerical modeling for this region at the acoustic pulse propagation time of 25×10^{-6} s.

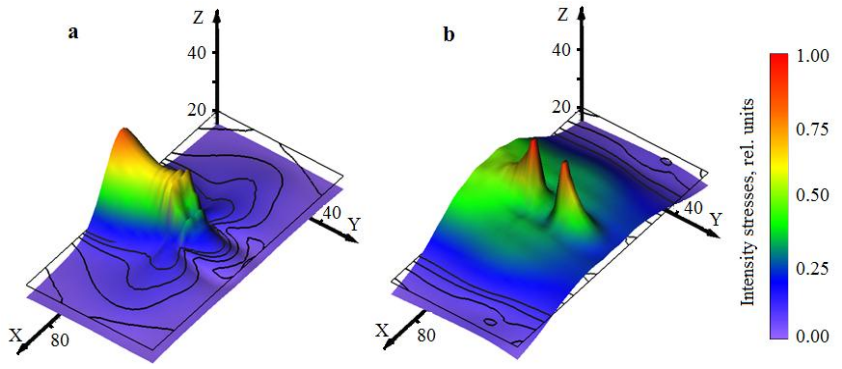

Figure 2. Calculated values of stress intensity in the sample bulk within 25×10^{-6} s from the moment of the acoustic pulse input by the ball impact on the cylindrical surface of the sample: a) crack 10^{-2} m long along the sample axis at a distance of 20×10^{-3} m from the excited cylindrical surface; b) crack 10^{-2} m long across the sample at a distance of 40×10^{-3} m from the face end of the sample under similar external impact.

In numerical modeling, changes in stress intensity over time from zero to 35×10^{-6} s were studied. For example, Figure 2a demonstrates changes in stress intensity in the bulk of the sample on a crack 10^{-2} m long located along the sample axis at a distance of 20×10^{-3} m from the excited cylindrical surface within 25×10^{-6} s from the moment of the acoustic pulse induced by the ball collision with the cylindrical surface. As can be seen in the figure, stresses are concentrated on the crack, and then they drop sharply along the line of AP propagation. As reported in the introduction, the amplitude-frequency spectrum of EMS is directly related to the parameters of the time-varying AP. As a result, the EMS spectrum also changes.

Figure 2b represents changes in stress intensity in the bulk of the sample on the crack 10^{-2} m long located across the sample axis at a distance of 40×10^{-3} m from the sample end face under similar external action from the excited cylindrical surface. The figure also presents the calculation of stresses within 25×10^{-6} s from the moment of the acoustic pulse input after the ball impact on the cylindrical surface. As can be seen in the

figure, stresses are concentrated on the crack, but their shape differs from the previous one (Figure 2a). Therefore, the EMS amplitude-frequency spectrum will be different. The form of the amplitude-frequency spectrum under deterministic acoustic excitation can help to determine the location of existing or emerging cracks during sample fracture propagation caused by different types of strength loading.

Figure 3 shows the results of numerical simulation of the change in the stress intensity in the region of the sample with dimensions $(42\times80)\times10^{-3}$ m^2 after 30×10^{-6} s from the moment of injection of a deterministic acoustic pulse in the middle of the surface perpendicular to the direction of uniaxial compression for a crack 10^{-2} meters, for two cracks 20×10^{-3} and 42×10^{-3} meters along the compression axis each at a distance of 10^{-2} meters from the edges of the sample, as well as for several cracks located along the compression axis with dimensions $(2.0, 4.0, 8.0, 16.0, 32.0, 64.0)\times10^{-3}$ meters, the distance between cracks is 5×10^{-3} m. In the latter case, the cracks are arranged in ascending order from the smallest in length to the largest from the point of application of the impulse.

In Figures 2 and 3, the intensity of the stresses arising in the sample is displayed in color. They show that cracks are stress concentrators. An electromagnetic signal with the highest amplitude will come from the area of such stress concentrations. The Z-axis in Figures 2 and 3 coincides with the direction of the maximum principal stress. Thus, in the process of any type of force action, electromagnetic emission will reflect the appearance of cracks and the development of zones of the destruction of materials.

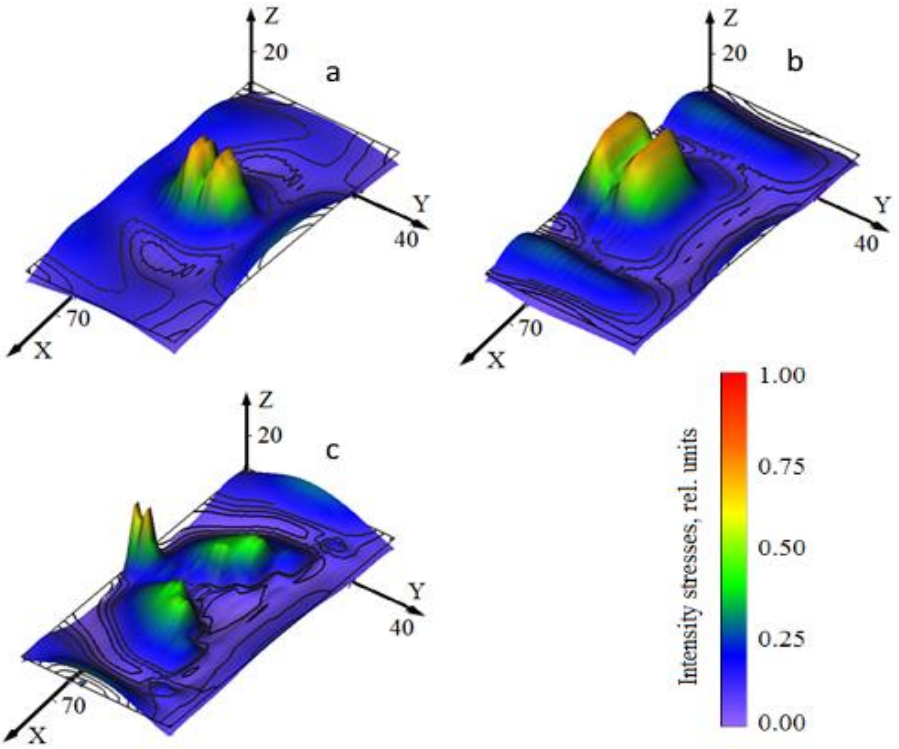

Figure 3. Numerical modeling of the stress intensity dynamic in a sample with dimensions $(42\times80)\times10^{-3}$ m^2 after 30×10^{-6} s from the moment of input of a deterministic acoustic pulse in the middle of the surface perpendicular to the direction of uniaxial compression: a) crack 10^{-2} m; b) two cracks 20×10^{-3} and 42×10^{-3} m along the compression axis each at a distance of 10^{-2} m from the edges of the sample; c) the area contains several cracks located along the compression axis with dimensions $(2.0, 4.0, 8.0, 16.0, 32.0, 64.0)\times10^{-3}$ m, the distance between the cracks is 5×10^{-3} m, the cracks are arranged in ascending order from the smallest to the largest one from the point of application of the impulse.

During the experiments, the electromagnetic emission of rock samples of skarn containing magnetite and magnetite ore of different strengths was investigated when they were loaded along the axis by uniaxial compression. Figure 4a shows the amplitudes of the EME skarn averaged over 1 second in a wide frequency band of 1 ... 100 kHz. The sample contained calcite and magnetite. The EME was recorded continuously with the recording of the current values of the compressive stresses P in the range from zero to destructive loading values P_{lim}. The figure shows the stages of the development of fracture, including the stage of devel-

opment of destruction of the sample material or the growth of primary cracks and their growth in the range of 0.3 ... 0.52 of the relative load.

The relative load is the ratio of the current load to the breaking load P/P_{lim}. Similar changes in the EME amplitude were observed during the development of destructive processes in magnetite ore (Figure 4b). It can be seen from the obtained regularities of the development of destruction at stage 2 that two independent increases in the EME amplitude are observed. This is due to the fact that when the samples are loaded with compressive forces, the resulting stresses are transmitted to their entire volume, including calcite and magnetite. Deformation in brittle materials obeys Hooke's law. As a result of such an impact, the most fragile material will be destroyed first.

Thus, various modifications of calcite, depending on its position and type in the rock, have a strength of $(12–50)\times10^6$ Pa, while the strength of magnetite ore is significantly higher. In this regard, the zone of destruction in the minerals that make up the rock will develop in different intervals of the relative load P/P_{lim}. This is shown in Figure 4 when loading skarn and magnetite ore samples. Summarizing the results of the study to identify the influence of the mineral composition of rock samples on the EME amplitude, we can say that the least durable inclusions present in the material will always initially undergo destruction.

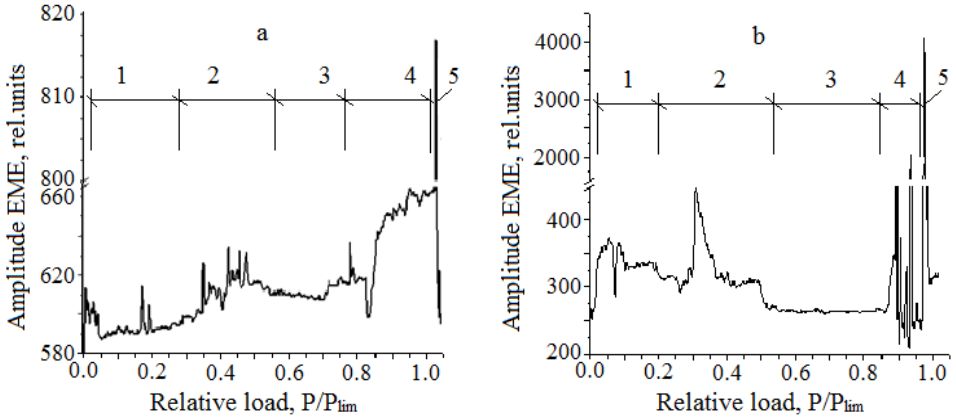

1 – compaction stage; 2 – destruction focus formation stage; 3 – sustainable strength stage; 4 – pre-destruction stage; 5 – growth of a tear-off crack

Figure 4. Changes in the EME amplitudes averaged over one second at a frequency of 100 kHz at different values of the relative compressive load on the sample: a) skarn; b) magnetite ore.

Conclusions

Analyzing the numerical calculations of the stress intensity on cracks of different sizes and locations, and the experimental regularities of the EME amplitude and frequency characteristics under uniaxial compression we concluded that some important features can be distinguished during testing the fracture processes development by the method of mechanical and electrical transformations.

Thus, the performed numerical simulation of the stress intensity dynamic in the samples under deterministic acoustic excitation at the middle of the surface perpendicular to the direction of uniaxial compression, revealed that the cracks in the sample volume are stress concentrators. The stress intensity and their type differ significantly with different numbers and sizes of cracks perpendicular to the propagation of the acoustic pulse. EMS with the highest amplitude and with different amplitude-frequency spectra will come from the region of such concentrations because the EMS parameters are related to the characteristics of the arising mechanical stresses.

The experimentally obtained results of EME during the uniaxial compression of skarn and magnetite ore samples of different strengths revealed the stages of preparation for the samples destruction. The emergence and development of destructive zones are in the range from 0.3 to 0.55 of the breaking load. It should be borne in mind that for different materials the interval of this range may vary depending on their strength. This circumstance indicates the depending on the EMS parameters from the samples structure and their dielectric properties under mechanical-electrical conversions.

Thus, the use of the mechanical-electrical method under compression will be useful in testing the processes of the cracks onset and the fracture development in solid dielectric materials and products. In the fu-

ture, the considered method can be used to detect defects in dielectric materials. The prerequisites for such defects testing are the above theoretical studies of changes in mechanical stresses in a model solid on defects in the form of cracks under an external deterministic acoustic effect. Cracks here are stress concentrators during the propagation of acoustic pulses. The same concentrators of mechanical stresses will be the contacts of defects with the material containing them. As a result, in accordance with the defect and the sample impedance ratio, EMS with parameters defining the defects boundaries will appear.

Acknowledgements

The work was done with the financial support of the Russian Science Foundation; Project No. 20-79-10156 (TPU - 19.0066.RNF.2020).

References

1 Воробьев А.А. Изменение электропроводности и радиоизлучение горных пород и минералов при физико-химических процессах в них / А.А. Воробьев, Е.К. Заводовская, В.Н. Сальников // Докл. АН СССР. — 1975. — 220. — № 1. — С. 82–85.

2 Misra A. Electromagnetic radiation characteristics during fatigue crack propagation and failure / A. Misra, S. Gosh // Appl. Phys. — 1980. — 23. — P. 387–390.

3 Хатиашвили Н. Г. Генерация электромагнитного излучения при прохождении акустических волн через кристаллические диэлектрики и некоторые горные породы / Н.Г. Хатиашвили, М.Е. Перельман // Докл. АН СССР. — 1982. — 263. — № 4. — С. 839–842.

4 Yamada I. Electromagnetic and acoustic emission associated with rock fracture / I. Yamada, K. Masuda, H. Mizutani // Phys. Earth Planet. Int. — 1989. — 57. — P. 157–168.

5 Ogawa T. Electromagnetic radiations from rocks / T. Ogawa, K. Oike, T. Miura // J. Geophys. Res. — 1985. — 90. — P. 6245–6249.

6 Dann D.D. Changes in the parameters of the electromagnetic response of model dielectric samples with air cavity defects under external deterministic acoustic impact / D. D. Dann, M.V. Petrov, P.I. Fedotov, E.A. Sheveleva // Bulletin of the university of Karaganda-Physics. — 2021. — 1. — P. 12–17.

7 Petrenko V.F. On the nature of electrical polarization of materials caused by cracks, application to ice / V.F. Petrenko // Philosophical Magazine B. — 1993. — 67. — No. 3. — P. 301–315.

8 A mechanism for the production of electromagnetic radiation during fracture of brittle materials / S.G. O'Keefe, D.V. Thiel // Phys. Earth and Planet. Inter. — 1995. — 89. — No. 11. — P. 127–135.

9 Беспалько А. А. Влияние электризации кальцитов на параметры электромагнитных сигналов при импульсном акустическом воздействии / А.А. Беспалько, Р.М. Гольд, Л.В. Яворович // Физическая мезомеханика. — 2004. — 7. — № 5. — С. 95–99.

10 Lacidogna G. Acoustic and electromagnetic emissions as precursor phenomena in failure processes / G. Lacidogna, A. Carpinteri, A. Manuello, G. Durin, A. Schiavi, G. Niccolini, A. Agosto // Strain. — 2010. — 47. — P. 144–152.

11 Bespal'ko A.A. Transformation of acoustic pulses into electromagnetic response in stratified and damaged structures / A.A. Bespal'ko, Y.N. Isaev, L.V. Yavorovich // Journal of Mining Science. — 2016. — 52. — No. 2. — P. 279–285.

12 Fursa T. Development prospects for nondestructive testing of heterogeneous nonmetallic materials by the parameters of electrical response to a shock action / T.V. Fursa, G.E. Utsyn, D.D. Dann, M.V. Petrov // Russian Journal of Nondestructive Testing. — 2017. — 53. — No. 2. — P. 104–110.

13 Bespal'ko A. Polarization and electromagnetic emissions of natural crystalline structures upon acoustic excitation / A. Bespal'ko, A. Surzhikov, P. Fedotov, E. Pomishin, O. Stary // Materials Science Forum. — 2019. — 970. — P. 153–166.

14 Физические свойства горных пород и минералов: справочник по геофизике. Петрофизика. — М.: Недра, 1976.

15 Добрынин В.М. Петрофизика: учеб. для вузов / В.М. Добрынин, Ю.Ю. Вендельштейн, Д.А. Кожевников. — М.: Недра, 1991.

16 Ziman J.M. Principles of the Theory of Solids / J.M. Ziman // Cambridge University Press. — London, 1972.

17 Давыдов А.С. Теория твердого тела / А.С. Давыдов. — М.: Наука, 1976.

18 Mason W.P. Physical Acoustics / W.P. Mason. — New York: Academic Press, 1964. — 1.

19 Hoffman J.D. Numerical methods for engineers and scientists / J.D. Hoffman. — New York: Marcel Dekker. Second ed., 2001.

20 Hairer E. Solving ordinary differential equations II: Stiff and differential-algebraic problems / E. Hairer, G. Wanner. — Berlin. New York: Springer-Verlag. Second ed., 1996.

21 Горшков А.Г. Теория эластичности и упругости: учеб. для вузов / А.Г. Горшков. — М.: ФИЗМАТЛИТ, 2002. — С. 416.

22 Molotnikov V. Theory of Elasticity and Plasticity / V. Molotnikov, A. Molotnikova // A Textbook of Solid Body Mechanics. Springer International Publishing, 2021.

А.А. Беспалько, Г.Е. Уцын, П.И. Федотов

Диэлектрлік материалдардағы деструктивті процестердің дамуы кезіндегі механикалық және электрлік түрлендірулерді сандық және тәжірибелік зерттеулер

Мақалада диэлектрлік тау жыныстарының үлгілері мысалында кернеулі-деформациялық күйдің өзгеруімен сынудың дамуын механикалық және электрлік сынау әдісі талқыланған. Айнымалы электромагниттік өрістердің пайда болу құбылысы қатты дене құрылымдарындағы механикалық және электрлік түрлендірулерге негізделген, олардың кернеулі-деформациялық күйі механикалық жүктеменің әсерінен сыналған материал ішіндегі акустикалық эмиссиямен бірге өзгереді. Авторлар әртүрлі құрамы мен текстурасы бар тау жыныстарының үлгілерінің импульстік детерминирленген акустикалық қозуы кезіндегі электромагниттік реакциялардың параметрлерінің өзгеруін сандық және тәжірибелік зерттеулердің нәтижелерін талқылаған. Детерминирленген акустикалық импульстар енгізілген перпендикуляр үлгі осінің бойымен және көлденеңінен орналасқан жарықтардағы кернеу концентрациясының математикалық есептеулерінің нәтижелері берілген. Әр түрлі беріктігі мен электрлік қасиеттері бар кальцит пен магнетит үлгілер жойылғанға дейінгі біросьті сығымдау кезіндегі электромагниттік эмиссияны эксперименттік зерттеудің нәтижелері көрсетілген. Үлгі көлеміндегі жарықтар кернеу концентраторлары болып табылады. Акустикалық импульстің таралуына перпендикуляр жарықтардың саны мен мөлшері әр түрлі болған кезде кернеулердің қарқындылығы және олардың сыртқы түрі айтарлықтай өзгереді. Бұл жағдай үлгілердің құрылымының және олардың диэлектрлік қасиеттерінің механикалық және электрлік түрлендірулердің нәтижелерін жазу кезінде электромагниттік сигналдардың параметрлеріне әсерін көрсетеді. Осылайша, сығымдау кезіндегі механикалық–электрлік түрлендірулердің әзірленген әдісін пайдалану қатты денелі диэлектрлік материалдар мен бұйымдарда жарықшақтардың пайда болу және сынулардың даму процестерін сынауда қолданылуы мүмкін.

Кілт сөздер: диэлектриктер, тау жыныстары, сандық модельдеу, акустикалық әсер ету, біросьті сығу, электромагниттік эмиссия, механоэлектрлік қайта құру, электромагниттік сигнал.

А.А. Беспалько, Г.Е. Уцын, П.И. Федотов

Численное и экспериментальное исследования механико-электрических преобразований при развитии деструктивных процессов в диэлектрических материалах

В статье обсужден метод механико-электрического тестирования развития разрушения при изменении напряженно-деформированного состояния на примере диэлектрических образцов горных пород. В основе явления возникновения переменных электромагнитных полей лежат механико-электрические преобразования в твердотельных структурах при изменении их напряженно-деформированного состояния под воздействием механической нагрузки, сопровождающейся акустической эмиссией внутри испытываемого материала. Авторами рассмотрены результаты численных и экспериментальных исследований изменения параметров электромагнитных откликов при импульсном детерминированном акустическом возбуждении образцов горных пород с различным составом и текстурой. Представлены результаты математических расчетов концентрации напряжений на трещинах, расположенных вдоль и поперек оси образца, перпендикулярно которой вводились детерминированные акустические импульсы. Показаны результаты экспериментальных исследований электромагнитной эмиссии при одноосном сжатии до разрушения образцов с содержанием кальцита и магнетита, обладающих разной прочностью и электрическими свойствами. Присутствующие в объеме образца трещины являются концентраторами напряжений. При разном количестве и размерах трещин, перпендикулярных распространению акустического импульса, интенсивность напряжений и их вид существенно различаются. Это обстоятельство указывает на влияние структуры образцов и их диэлектрических свойств на параметры электромагнитных сигналов при регистрации результатов механико-электрических преобразований. Таким образом, использование метода механико-электрических преобразований при сжатии может быть использовано при тестировании процессов начала трещинообразования и развития разрушения в твердотельных диэлектрических материалах и изделиях.

Ключевые слова: диэлектрики, горные породы, численное моделирование, акустическое воздействие, одноосное сжатие, электромагнитная эмиссия, механоэлектрические преобразования, электромагнитный сигнал.

References

1 Vorobyov, A.A., Zavodovskaya, E.K., & Salnikov, V.N. (1975). Izmenenie elektroprovodnosti i radioizluchenie gornykh porod i mineralov pri fiziko-khimicheskikh protsessakh v nikh [Changes in electrical conductivity and radio emission of rocks and minerals during physical and chemical processes in them]. *Doklady Akademii nauk SSSR – Reports of USSR Academy of Sciences, 220 (1),* 82–85 [in Russian].

2 Misra, A., & Gosh, S. (1980). Electromagnetic radiation characteristics during fatigue crack propagation and failure. *Appl. Phys., 23,* 387–390.

3 Khatiashvili, N.G., & Perelman, M.E. (1982). Generatsiia elektromagnitnogo izlucheniia pri prokhozhdenii akusticheskikh voln cherez kristallicheskie dielektriki i nekotorye gornye porody [Generation of electromagnetic radiation when acoustic waves pass through crystal dielectrics and some rocks]. *Doklady Akademii nauk SSSR – Reports of USSR Academy of Sciences, 263(4),* 839–842 [in Russian].

4 Yamada, I., Masuda, K., & Mizutani, H. (1989). Electromagnetic and acoustic emission associated with rock fracture. *Phys. Earth Planet. Int., 57,* 157–168.

5 Ogawa, T., Oike, K., & Miura, T. (1985). Electromagnetic radiations from rocks. *J. Geophys. Res. 90,* 6245–6249.

6 Dann, D.D., Petrov, M.V., Fedotov, P.I., & Sheveleva, E.A. (2021). Changes in the parameters of the electromagnetic response of model dielectric samples with air cavity defects under external deterministic acoustic impact. *Bulletin of the university of Karaganda-Physics, 1,* 12–17.

7 Petrenko, V.F. (1993). On the nature of electrical polarization of materials caused by cracks, application to ice. *Philosophical Magazine B, 67, 3,* 301–315.

8 O'Keefe, S.G. & Thiel, D.V. (1995). A mechanism for the production of electromagnetic radiation during fracture of brittle materials. *Phys. Earth and Planet. Inter, 89(11),* 127–135.

9 Bespalko, A.A., Gold, R.M., & Yavorovich, L.V. (2004). Vliianie elektrizatsii kaltsitov na parametry elektromagnitnykh signalov pri impulsnom akusticheskom vozdeistvii [Influence of calcite electrification on parameters of electromagnetic signals under pulsed acoustic influence]. *Fizicheskaia mezomekhanika — Physical mesomechanics, 7(5),* 95–99 [in Russian].

10 Lacidogna, G., Carpinteri, A., Manuello, A., et.al. (2010). Acoustic and electromagnetic emissions as precursor phenomena in failure processes. *Strain, 47,* 144–152.

11 Bespal'ko, A.A., Isaev, Y.N., & Yavorovich, L.V. (2016). Transformation of acoustic pulses into electromagnetic response in stratified and damaged structures. *Journal of Mining Science, 52, 2,* 279–285.

12 Fursa, T.V., Utsyn, G.E., Dann, D.D., & Petrov, M.V. (2017). Development prospects for nondestructive testing of heterogeneous nonmetallic materials by the parameters of electrical response to a shock action. *Russian Journal of Nondestructive Testing, 53(2),* 104–110.

13 Bespalko, A., Surzhikov, A., Fedotov, P., Pomishin, E., & Stary, O. (2019). Polarization and electromagnetic emissions of natural crystalline structures upon acoustic excitation. *Materials Science Forum, 970,* 153–166.

14 Fizicheskie svoistva gornykh porod i mineralov [Physical properties of rocks and minerals] (1976): *Spravochnik po geofizike. Petrofizika — Handbook of Geophysics. Petrophysics.* Moscow: Nedra [in Russian].

15 Dobrynin, V.M., Vendelstein, Yu.Yu., & Kozhevnikov, D.A. (1991). *Petrofizika: uchebnik dlia vuzov — Petrophysics: textbook for universities.* Moscow: Nedra [in Russian].

16 Ziman, J.M. (1972). *Principles of the Theory of Solids.* Cambridge University Press, London.

17 Davydov, A.S. (1976). *Teoriia tverdogo tela [Theory of a solid body]*. Moscow: Nauka [in Russian].

18 Mason, W.P. (1964). *Physical Acoustics.* New York: Academic Press, 1.

19 Hoffman, J.D. (2001). *Numerical methods for engineers and scientists. Second edition revised and expanded*. New York: Marcel Dekker, Inc.

20 Hairer, E., & Wanner, G. (1996). *Solving ordinary differential equations II: Stiff and differential-algebraic problems. Second edition.* Berlin, New York: Springer-Verlag,

21 Gorshkov, A.G., Starovoitov, E.I., & Tarlakovsky, D.V. (2002). *Teoriia elastichnosti i uprugosti [Theory of elasticity and plasticity]*. Moscow: FIZMATLIT [in Russian].

22 Molotnikov, V., & Molotnikova, A. (2021). *Theory of Elasticity and Plasticity. A Textbook of Solid Body Mechanics.* Springer International Publishing.